Driven-dissipative quantum battery with nonequilibrium reservoirs

Zhihai Wang[1,2], Hongwei Yu[1] and Jin Wang[3*]

1 State Key Laboratory of Electroanalytical Chemistry, Changchun Institute of Applied Chemistry, Chinese Academy of Sciences, Changchun 130022, China
2 Center for Quantum Sciences and School of Physics, Northeast Normal University, Changchun 130024, China
3 Department of Chemistry and Department of Physics and Astronomy, State University of New York at Stony Brook, New York 11794, USA
* jin.wang.1@stonybrook.edu

November 20, 2024

Abstract

We investigate a quantum battery system under both external driving and dissipation. The system consists of a coupled two-level charger and battery immersed in nonequilibrium fermionic reservoirs. By considering the changes in the energy spectrum induced by external driving and charger-battery coupling in a non-perturbative manner, we go beyond the secular approximation to derive the Redfield master equation. In the nonequilibrium scenario, both charging efficiency and power of the quantum battery can be optimized through a compensation mechanism. **When the charger and battery are off-resonance, a significant chemical potential difference between the reservoirs, which characterizes the degree of nonequilibrium, plays a crucial role. Specifically, the charger's frequency should be higher (lower) than that of the battery when the average chemical potential is negative (positive) to achieve enhanced charging efficiency and power under strong nonequilibrium conditions. Remarkably, the efficiency in the nonequilibrium case can surpass that in the equilibrium setup. Our results provide insights into the design and optimization of quantum batteries in nonequilibrium open systems.**

1 Introduction

A central challenge in quantum technology is to explore how quantum resources can be utilized to perform tasks that are unattainable with classical systems. One such task arises in the realm of energy storage, giving rise to the concept of the "quantum battery." A typical quantum battery system consists of a charger, which supplies energy, and a battery, which stores and releases the energy.

Ever since the concept of the quantum battery was introduced by Alicke and Fannes [1], numerous quantum battery models have been proposed in various physical systems. Examples include spin or resonator chain models [2–15], the Tavis-Cummings and Dicke models in quantum optics [16–21], and Rydberg atom systems [22]. In some of these systems, Floquet engineering has been employed to enhance the performance of quantum batteries [23–25]. Given that quantum systems are inherently coupled to their environments, quantum batteries in open systems are now drawing increasing attention [26–36].

The simplest open system for a quantum battery is perhaps a setup involving two coupled two-level systems, each interacting with external environments. One of these systems, driven by a classical field, acts as the charger, while the other serves as the battery [28]. To explore how particle exchange between the system and reservoirs impacts the quantum battery's performance, we further couple the charger and battery to two independent fermionic reservoirs. The nonequilibrium effect is characterized by the chemical potential difference between these reservoirs. In this quantum open system, the external driving applied to the charger provides energy to the system, necessitating a reassessment of efficiency. Moreover, the nonequilibrium nature of the reservoirs plays a crucial role in shaping the steady-state properties of the system.

To analyze the effects of driving and nonequilibrium effects on the performance of the quantum battery, we employ a quantum master equation approach under the Born-Markovian approximation [37]. Classical driving significantly alters the energy spectrum of the charger-battery system. However, in the conventional Lindblad master equation approach, driving is treated as a perturbation, its impact on the system's energy spectrum is neglected, and the injected energy is not fully considered when evaluating the efficiency of the quantum battery. To address these limitations, we go beyond the Lindblad master equation and adopt the Redfield master equation [38, 39], which has been extensively used in studies of quantum transport [40, 41] and photosynthetic processes [42–44]. Specifically, we work in the eigen state representation by considering the case of strong coupling between the driving field and the system, thus treating the driving field as an integral part of the open system rather than as a perturbation. This approach allows us to define the charging efficiency and power in a consistent manner. This methodology contrasts sharply with the traditional treatment [28], where the driving is modeled phenomenologically as an effective reservoir weakly coupled to the system. Additionally, we consider the nonequilibrium effects characterized by the chemical potential difference between the two reservoirs coupled to the system. Such nonequilibrium has been shown to induce steady-state coherence and entanglement [45–55]. By moving beyond the secular approximation, we investigate whether the nonequilibrium
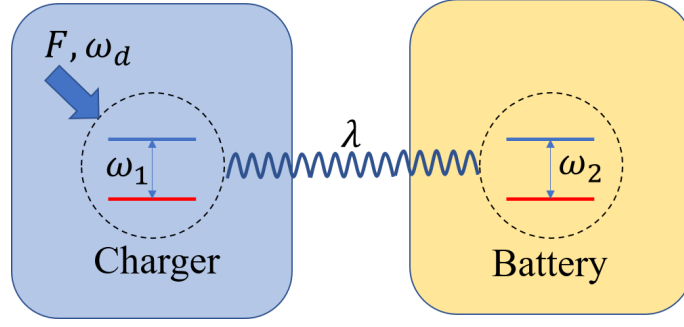
Figure 1: Schematic diagram of the quantum battery model under consideration. The charger and the battery are modeled as two-level systems with transition frequencies ω_1 and ω_2, respectively. Each system is coupled to its individual reservoir and they interact with each other via a coupling strength λ. The charger is driven by an external classical field with driving strength F and frequency ω_d.

reservoirs can enhance the performance of the quantum battery.

Using the Redfield master equation, we uncover a compensation mechanism that enhances the charging efficiency and power of the quantum battery. Specifically, the charger's frequency should exceed that of the battery when the average chemical potential is sufficiently negative and large. Under these conditions, the maximum efficiency can exceed 90% significantly surpassing the efficiency achievable in the equilibrium case. Moreover, this compensation mechanism is also effective in boosting the charging power of the quantum battery.

The rest of the paper is organized as follows. In Sec. 2, we illustrate our model and derive the Redfield master equation. In Sec. 3, we discuss the steady state entanglement in our system. The charging efficiency and power of quantum battery are investigated in Sec. 4 and Sec. 5, respectively. At last, we give a short conclusion in Sec. 6.

2 Model and master equation

As schematically illustrated in Fig. 1, the quantum battery system under consideration consists of a charger and a battery, both modeled as two-level systems. The charger is driven by a classical field, and both the charger and the battery are coupled to their respective reservoirs, which obey fermionic statistics. In the rotating frame with respect to the driving field frequency ω_d, the Hamiltonian of the entire system, including the reservoirs, is given by $H = H_s + H_B + V$.

The Hamiltonian for the charger-battery system is [28] ($\hbar = k_B = 1$ in what follows)

$$H_s = \frac{\omega_1}{2}\sigma_z^{(1)} + \frac{\omega_2}{2}\sigma_z^{(2)} + \lambda\left(\sigma_+^{(1)}\sigma_-^{(2)} + \sigma_-^{(1)}\sigma_+^{(2)}\right) + \frac{F}{2}\left(\sigma_+^{(1)}e^{-i\omega_d t} + \sigma_-^{(1)}e^{i\omega_d t}\right). \quad (1)$$

Here, $\sigma_m^{(i)}(m = z, +, -)$ represents the Pauli operators for the i-th two-level system with transition frequency ω_i. The indices 1 and 2 correspond to the charger and the battery, respectively. The driving field has a frequency ω_d, F denotes the driving strength, and λ represents the coupling strength between the charger and the battery.

The Hamiltonian of the reservoirs is given by

$$H_B = \sum_k \omega_{bk} b_k^\dagger b_k + \sum_k \omega_{ck} c_k^\dagger c_k, \quad (2)$$

where b_k ($b_k^\dagger$) and c_k ($c_k^\dagger$) are the annihilation (creation) operators for the kth mode with frequencies ω_{bk} and ω_{ck} in the reservoirs coupled to the charger and the battery, respectively.

The Hamiltonian describing the system-reservoir coupling is expressed as

$$
V = \sum_k g_k \left(\sigma_-^{(1)} b_k^\dagger + \sigma_+^{(1)} b_k \right) + \sum_k f_k \left(\sigma_-^{(2)} c_k^\dagger + \sigma_+^{(2)} c_k \right),
\tag{3}
$$

where g_k (f_k) denotes the coupling strength between the charger (battery) and the kth mode in its respective reservoir.

The time dependence of the Hamiltonian can be eliminated by working in the rotating frame defined by $U_1(t) = \exp\left[i\omega_d \left(\frac{\sigma_z^{(1)} + \sigma_z^{(2)}}{2} + \sum_k (b_k^\dagger b_k + c_k^\dagger c_k) \right) t \right]$.

In this rotating frame, the Hamiltonian becomes

$$
H_s = \frac{\Delta_1}{2}\sigma_z^{(1)} + \frac{\Delta_2}{2}\sigma_z^{(2)} + \lambda \left(\sigma_+^{(1)}\sigma_-^{(2)} + \sigma_-^{(1)}\sigma_+^{(2)} \right) + \frac{F}{2}\left(\sigma_+^{(1)} + \sigma_-^{(1)} \right),
\tag{4}
$$

$$
H_B = \sum_k (\omega_{bk} - \omega_d) b_k^\dagger b_k + \sum_k (\omega_{ck} - \omega_d) c_k^\dagger c_k,
\tag{5}
$$

where $\Delta_i = \omega_i - \omega_d$, and the interaction Hamiltonian V remains unchanged due to the application of the rotating wave approximation.

With these significant approximations and simplifications, the conventional Markovian master equation for the charger-battery system can be written as

$$
\frac{d}{dt}\rho = -i[H_s, \rho] + \sum_{i=1}^{2} J_i(\omega_i) N_i(\omega_i) D_{\sigma_+^{(i)}}[\rho] + \sum_{i=1}^{2} J_i(\omega_i) \mathcal{N}_i(\omega_i) D_{\sigma_-^{(i)}}[\rho],
\tag{6}
$$

where $D_A[\rho] = 2A\rho A^\dagger - A^\dagger A\rho - \rho A^\dagger A$, $J_1(\omega) = \pi \sum_k g_k^2 \delta(\omega - \omega_{bk})$ and $J_2(\omega) = \pi \sum_k f_k^2 \delta(\omega - \omega_{ck})$ are the spectral densities of the two reservoirs.

For the fermionic reservoirs, the average particle number at frequency ω in the ith reservoir is $N_i(\omega) = \frac{1}{\exp[(\omega - \mu_i)/T_i] + 1}$, where μ_i and T_i are the chemical potential and temperature of the ith reservoir, respectively, and $\mathcal{N}_i(\omega) = 1 - N_i(\omega)$.

Actually, in writing the above master equation, one only simply adds the dissipation terms of the charger and the battery. As a result, the master equation yields a Lindblad form. We should note that both of the driving to the charger and the charger-battery coupling will affect the eigen spectrum of the system, compared to the case when both of the charger and the battery are free. In what follows, we will derive the master equations by taking into account of both of the strong driving and coupling effects and obtain the Redfield master equations.

2.1 Redfield master equation

To obtain the Redfield master equation, we first solve the eigen energies and corresponding eigen states of the Hamiltonian given by Eq. (4). This is achieved numerically, and the results are expressed as

$$
H_s = \sum_{i=1}^{4} E_i |E_i\rangle\langle E_i|,
\tag{7}
$$

where the eigen energies are ordered as $E_1 > E_2 > E_3 > E_4$, and $|E_i\rangle$ represents the corresponding eigen state.

In terms of the eigen states, we have

$$\sigma_-^{(m)} = \sum_{i,j=1}^{4} \chi_{ij}^{(m)} \tau_{ij}, \qquad (8)$$

where $\tau_{ij} = |E_i\rangle\langle E_j|$, and $\chi_{ij}^{(m)} = \langle E_i|U\sigma_-^{(m)}U^\dagger|E_j\rangle$ for $m = 1, 2$. The unitary transformation U, obtained via numerical diagonalization of the Hamiltonian H_s, connects the eigen states with the bare states.

The relationships between the eigen states and bare states are given by

$$(|E_1\rangle, |E_2\rangle, |E_3\rangle, |E_4\rangle)^T = U(|ee\rangle, |eg\rangle, |ge\rangle, |gg\rangle)^T, \qquad (9a)$$

$$(|ee\rangle, |eg\rangle, |ge\rangle, |gg\rangle)^T = U^\dagger(|E_1\rangle, |E_2\rangle, |E_3\rangle, |E_4\rangle)^T. \qquad (9b)$$

By redefining the bare basis of the charger-battery system as $|1\rangle = |ee\rangle$, $|2\rangle = |eg\rangle$, $|3\rangle = |ge\rangle$, and $|4\rangle = |gg\rangle$, the elements of the transformation matrix U are expressed as $U_{ij} = \langle E_i|j\rangle$.

As a result, the interaction Hamiltonian in the interaction picture can be written as

$$V = \sum_{i,j>i} \sum_{k} \left(g_k \chi_{ij}^{(1)} b_k \tau_{ij} e^{-i(\omega_{bk} - \omega_{ji})t} + f_k \chi_{ij}^{(2)} c_k \tau_{ij} e^{-i(\omega_{ck} - \omega_{ji})t} + \text{H.c.} \right), \qquad (10)$$

where we have applied the rotating wave approximation again, considering that the system weakly couples to the reservoirs.

Using the general form of the master equation [37],

$$\frac{d}{dt}\rho^{(I)} = -\int_0^\infty d\tau \, \text{Tr}_B \left[V_I(t), \left[V_I(t-\tau), \rho^{(I)} \otimes \rho_B^{(I)} \right] \right], \qquad (11)$$

where the superscript I indicates the interaction picture (while the absence of a superscript refers to the Schroedinger picture), the master equation under the Markovian approximation for our system reads

$$\frac{d}{dt}\rho = \mathcal{L}\rho = -i \left[\sum_{j=1}^{4} E_j|E_j\rangle\langle E_j|, \rho \right] + \mathcal{D}_1(\rho) + \mathcal{D}_2(\rho), \qquad (12)$$

where

$$\mathcal{D}_1(\rho) = \sum_{i,j>i} \sum_{m,n>m} \sum_{\alpha=1,2} J_\alpha(\epsilon_{mn}) \mathcal{N}_\alpha(\epsilon_{mn}) \mathcal{G}_{ij,mn}^{(\alpha)}[\rho], \qquad (13)$$

$$\mathcal{D}_2(\rho) = \sum_{i,j>i} \sum_{m,n>m} \sum_{\alpha=1,2} J_\alpha(\epsilon_{mn}) N_\alpha(\epsilon_{mn}) \mathcal{H}_{ij,mn}^{(\alpha)}[\rho], \qquad (14)$$

and

$$\mathcal{G}_{ij,mn}^{(\alpha)}[\rho] = \chi_{ji}^{(\alpha)}\chi_{mn}^{(\alpha)} \left(\tau_{ji}\rho\tau_{mn} - \rho\tau_{mn}\tau_{ji} \right) + \chi_{ij}^{(\alpha)}\chi_{nm}^{(\alpha)} \left(\tau_{nm}\rho\tau_{ij} - \tau_{ij}\tau_{nm}\rho \right), \quad (15)$$

$$\mathcal{H}_{ij,mn}^{(\alpha)}[\rho] = \chi_{ij}^{(\alpha)}\chi_{nm}^{(\alpha)} \left(\tau_{ij}\rho\tau_{nm} - \rho\tau_{nm}\tau_{ij} \right) + \chi_{ji}^{(\alpha)}\chi_{mn}^{(\alpha)} \left(\tau_{mn}\rho\tau_{ji} - \tau_{ji}\tau_{mn}\rho \right). \quad (16)$$

One should note that, since the charger and the battery are immersed in fermionic reservoirs characterized by different chemical potentials which creates nonequilibrium conditions, we have gone beyond the commonly used secular approximation in the above Redfield master equation. This is achieved by including the summation terms with $\epsilon_{mn} \neq \epsilon_{ij}$, which correspond to fast oscillating terms in the interaction picture. In our previous works [50, 52], we demonstrated that these non-secular terms give rise to steady-state coherence, a feature that is absent in equilibrium open systems.

2.2 Basic concept for quantum battery

In the eigen state representation, the initial state is given by $|\psi(0)\rangle_e = U^\dagger|\psi(0)\rangle$, and the system undergoes time evolution governed by the master equation in Eq. (12). After a time interval τ, at which the charging process is assumed to end, the system reaches a state with density matrix $\rho(\tau)$. Returning to the bare representation and the Schroedinger picture, we have

$$\tilde{\rho}(\tau) = U_1(\tau)U\rho(\tau)U^\dagger U_1^\dagger(\tau), \tag{17}$$

where $U_1(\tau) = \exp[i\omega_d(\sigma_z^{(1)} + \sigma_z^{(2)})\tau/2]$ is defined by the rotating frame, and U is the unitary transformation connecting the bare state representation and the eigen state representation.

We formally assume that $\tilde{\rho}(\tau)$ can be expressed as (in the basis of $\{|ee\rangle, |eg\rangle, |ge\rangle, |gg\rangle\}$)

$$\tilde{\rho}(\tau) = \begin{pmatrix} M_{11} & M_{12} & M_{13} & M_{14} \\ M_{21} & M_{22} & M_{23} & M_{24} \\ M_{31} & M_{32} & M_{33} & M_{34} \\ M_{41} & M_{42} & M_{43} & M_{44} \end{pmatrix}, \tag{18}$$

and the reduced density matrix for the battery subsystem can be expressed as (in the basis of $\{|e\rangle, |g\rangle\}$)

$$\rho_B = \begin{pmatrix} M_{33} + M_{11} & M_{12} + M_{34} \\ M_{21} + M_{43} & M_{44} + M_{22} \end{pmatrix}. \tag{19}$$

In the quantum battery scenario, one of the key quantities of interest is the mean charging energy E_B stored in the battery at the end of the charging process, which is expressed as [56, 57]

$$E_B(\tau) = \text{Tr}[H_B\rho_B(\tau)] - \text{Tr}[H_B\rho_B(0)], \tag{20}$$

where $H_B = \omega(|e\rangle\langle e| - |g\rangle\langle g|)/2$. The corresponding average energy per unit time, i.e., the charging power, is given by $P(\tau) = E_B(\tau)/\tau$. Another quantity of interest is the ergotropy function $\mathcal{E}_B$, which has a clear physical interpretation as follows.

Considering the state of a quantum system, characterized by the free Hamiltonian H, is given by the density matrix ρ. Using spectral decomposition, ρ and H can be expressed as

$$\rho = \sum_n r_n|r_n\rangle\langle r_n|, \quad H = \sum_n e_n|e_n\rangle\langle e_n|, \tag{21}$$

where r_n and e_n are the eigen values of ρ and H, with corresponding eigen states $|r_n\rangle$ and $|e_n\rangle$. By arranging the eigen values such that $r_0 \geq r_1 \geq r_2 \geq \cdots$ and $e_0 \leq e_1 \leq e_2 \leq \cdots$, we can construct a quantum state with a density matrix given by

$$\rho^{(p)} = \sum_n r_n|e_n\rangle\langle e_n|. \tag{22}$$

When a quantum system is in such a state, it cannot release energy to its surroundings. Therefore, the state $\rho^{(p)}$ is referred to as a passive state [56, 57]. The energy of the passive state is given by

$$E^{(p)} = \text{Tr}(H\rho^{(p)}) = \sum_n r_n e_n, \tag{23}$$

which can also be expressed as

$$E^{(p)} = \min_{U_B} \text{Tr}[H U_B \rho_B(\tau) U_B^\dagger]. \tag{24}$$

Here, the minimization is performed over all local unitary transformations U_B acting on the battery subsystem. This represents the portion of energy in $E_B(\tau)$ that is locked in correlations within the system, making it inaccessible through local operations on the battery.

Thus, the ergotropy, which represents the extractable energy from the battery, is defined as

$$\mathcal{E}_B(\tau) = E_B(\tau) - E^{(p)}. \tag{25}$$

For our two-level battery system, the above quantities can be calculated as [28]

$$
\begin{aligned}
E_B(\tau) &= \frac{\omega}{2}(N+1), &\tag{26}\\
\mathcal{E}_B(\tau) &= \frac{\omega}{2}\left(\sqrt{\langle\sigma_z\rangle^2 + 4\langle\sigma_+\rangle\langle\sigma_-\rangle} + \langle\sigma_z\rangle\right)\\
&= \frac{\omega}{2}\left(\sqrt{N^2 + 4|\mathcal{N}|^2} + N\right), &\tag{27}
\end{aligned}
$$

where $N = M_{11} + M_{33} - M_{22} - M_{44}$ and $\mathcal{N} = M_{12} + M_{34}$.

In what follows, we will first demonstrate the entanglement between the charger and the battery. Next, we will discuss the charging efficiency $R(\tau) = \mathcal{E}_B(\tau)/E_B(\tau)$ and the average power $P(\tau) = E_B(\tau)/\tau$.

3 Steady state entanglement

Under the combined effects of coherent driving by the classical field and dissipation induced by two non-equilibrium reservoirs, the charger-battery coupled system eventually reaches a steady state. This steady state is generally a mixed state but exhibits a certain degree of entanglement.

In the pioneering work of Hill and Wootters [58], the entanglement of an arbitrary two-qubit state ρ is quantified by the so-called concurrence. The concurrence is defined as $\mathcal{C} = \max\{0, \lambda_1 - \lambda_2 - \lambda_3 - \lambda_4\}$, where $\lambda_1 > \lambda_2 > \lambda_3 > \lambda_4$ are the eigen values of the matrix $\tilde{\rho} = (\sigma_y \otimes \sigma_y)\rho^*(\sigma_y \otimes \sigma_y)$, evaluated in the basis $\{|ee\rangle, |eg\rangle, |ge\rangle, |gg\rangle\}$. The concurrence $\mathcal{C}$ takes values between 0 and 1: the state is separable if $\mathcal{C} = 0$, while it is maximally entangled if $\mathcal{C} = 1$.

Without loss of generality, we choose the Ohmic spectral density given by

$$J_i(\omega) = \alpha_i \omega \exp(-\omega/\omega_c), \tag{28}$$

for $i = 1, 2$. In Fig. 2(a), we plot the steady-state concurrence $\mathcal{C}_{ss}$ between the charger and the battery as a function of their detuning $\Delta = \Delta_1 - \Delta_2$, considering both equilibrium and non-equilibrium scenarios where the two reservoirs share the same temperature. To evaluate any physical quantity A at steady state, denoted as $A_{ss} = A(\tau = \infty)$, we set $\tau = 20000/\lambda$. We have verified that the system achieves its steady state within this time interval.

For the equilibrium case of $\Delta\mu = 0$, the concurrence remains consistently very small ($\mathcal{C}_{ss} < 0.05$) as shown in Fig. 2(a), indicating that the charger and the battery are nearly separable. In contrast, non-zero entanglement can be observed when the frequency of the charger exceeds that of the battery for both $\Delta\mu > 0$ and $\Delta\mu < 0$. This suggests that driving the charger at a higher frequency facilitates the generation of steady-state entanglement. Moreover, the maximum steady-state concurrence achieved for $\Delta\mu < 0$ surpasses that for $\Delta\mu > 0$.

(a) (b) (c)
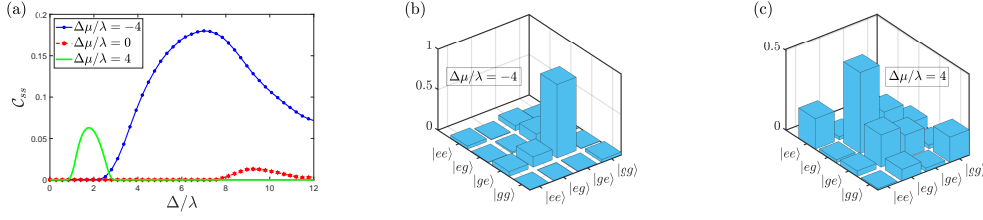
Figure 2: (a) The concurrence of the steady states governed by the Redfield master equation under fermion reservoirs. (b) and (c) Tomography of the steady states under nonequilibrium fermion reservoirs, where Δ is chosen such that the corresponding concurrence reaches its maximum value. The parameters are set as $F = 0.5\lambda$, $\omega_c = 5\lambda$, $T_1 = T_2 = \lambda$, $\bar{\mu} = 2\lambda$, and $\alpha_1 = \alpha_2 = 0.1\lambda$.

In the nonequilibrium case, the concurrence exhibits a non-monotonic behavior as a function of Δ. In particular, we tomograph the steady state when the concurrence reaches its maximum value for $\Delta\mu/\lambda = \pm 4$, as shown in Figs. 2(b) and (c). For the negative chemical potential difference, depicted in Fig. 2(b), the steady state predominantly occupies the superposition states of $|eg\rangle$ and $|ge\rangle$. Conversely, in Fig. 2(c), the mixing of the $|ee\rangle$ and $|gg\rangle$ states for $\Delta\mu > 0$ suppresses the concurrence of the charger-battery system.

4 Efficiency of the quantum battery

In this section, we will discuss the efficiency R_{ss} of the quantum battery setup by considering that the reservoirs are characterized by the Ohmic spectrum in Eq. (28).

Firstly, we consider the case where the charger and the battery are resonant, and the charger is resonantly driven. Furthermore, the charger and the battery are immersed in equilibrium reservoirs, characterized by $T_1 = T_2 = T$, $\mu_1 = \mu_2 = \mu$, and $\Delta_1 = \Delta_2 = 0$.

In Fig. 3(a), we plot the steady-state efficiency as a function of the chemical potential μ for different temperatures T. The results indicate that the efficiency drops off at a specific value of μ, which is slightly greater than 0 and independent of T. A possible explanation for this behavior is that when the chemical potentials of reservoirs are both near zero, they cannot exchange the particles with the charger-battery system, resulting in a low (or possibly zero) efficiency. The slight deviation observed may originate from the external driving of the charger. Additionally, as μ becomes sufficiently positive or negative, the efficiency saturates at a relatively large value, regardless of the temperature.

In Fig. 3(b), we investigate the efficiency as a function of temperature for different chemical potentials. At very low temperatures, the efficiency is nearly independent of T. However, as the temperature increases, the efficiency drops sharply and eventually approaches zero. This indicates that high temperatures degrade the performance of the battery due to thermal fluctuations.

Next, we consider more general cases where the charger and the battery are not resonant, and the two reservoirs are not in equilibrium. In Fig. 4, we plot the efficiency R_{ss} as a function of the chemical potential difference and the charger-battery detuning for different average chemical potentials $\bar{\mu} = (\mu_1 + \mu_2)/2$.

For small $\bar{\mu}$, such as $\bar{\mu} = 0$ and $\bar{\mu} = 3\lambda$, the maximum efficiency is achieved in the parameter regime with either $\Delta > 0$ or $\Delta < 0$ ($\Delta = \Delta_1 - \Delta_2$, the frequency difference between the charger and the battery) under significant chemical potential difference
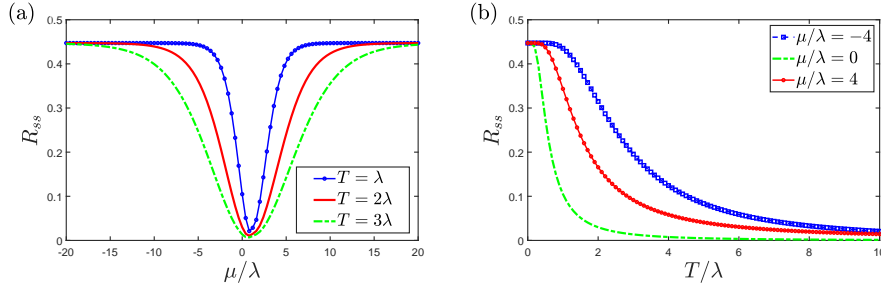
Figure 3: The efficiency R_{ss} as a function of $\mu_1 = \mu_2 = \mu$ (a) and $T_1 = T_2 = T$ (b) in equilibrium fermion reservoirs. The parameters are set as $F = 0.5\lambda$, $\omega_c = 5\lambda$, $\Delta_1 = \Delta_2 = 0$, and $\alpha_1 = \alpha_2 = 0.1\lambda$.

or nonequilibrium, as shown in Figs. 4(a) and (b). For a positively large $\bar{\mu} = 6\lambda$, the optimal regime shifts primarily to $\Delta < 0$, as depicted in Fig. 4(c). In stark contrast, when $\bar{\mu} = -6\lambda$, the optimal regime transitions to $\Delta > 0$ as seen in Fig. 4(d).

These behaviors can be intuitively explained by the compensation mechanism. When the chemical potential is negative, the charger-battery system tends to release particles to the environment. To compensate for this particle loss and achieve higher efficiency, the charger frequency should be higher than that of the battery ($\Delta > 0$). Conversely, when the chemical potential is positive, the charger frequency should be lower than the battery ($\Delta < 0$). Thus, the highest efficiency is achieved in the regime $\Delta > 0$ for $\bar{\mu} < 0$ (Fig. 4(d)) and in the regime $\Delta < 0$ for $\bar{\mu} > 0$ (Fig. 4(c)). For small $\bar{\mu}$ and $\Delta\mu$, the highest efficiency can appear in both $\Delta > 0$ and $\Delta < 0$ regimes (Figs. 4(a) and (b)), as particle flows between the charger and battery can either align (both release or absorb particles) or oppose (one releases while the other absorbs).

The results in Fig. 4 also demonstrate how to manipulate nonequilibrium characterized by the chemical potential difference between the reservoirs to enhance the charging efficiency of the quantum battery. When $\bar{\mu}$ is zero or positive, the maximum efficiency is predominantly localized in the regime $\Delta < 0$ under significant chemical potential difference (Figs. 4(a-c)). However, when $\bar{\mu}$ is negative, such as $\bar{\mu} = -6\lambda$, the role of nonequilibrium becomes negligible for enhancing efficiency.

From the results in Fig. 4, we observe that the efficiency at resonance ($\Delta = 0$) is always below 50%. However, this efficiency can exceed 90% when the charger is driven non-resonantly ($\Delta \neq 0$). Therefore, non-resonant driving proves to be a more effective strategy for enhancing the performance of the quantum battery in our setup.

5 Charging power

In the battery scenario, the charging power $P(\tau) = E(\tau)/\tau$ is another key quantity of interest. It describes the "velocity" of the charging process, as $E(\tau)$ represents the energy transferred to the battery from the charger. In Figs. 5(a) and (b), we analyze the charging power in both equilibrium and nonequilibrium cases.

In the equilibrium case, the results shown in Fig. 5(a) indicate that both the chemical potential and the temperature have minimal impact on the charging power. This suggests that an equilibrium system alone cannot effectively enhance the charging power. Fortunately, this limitation can be addressed by transitioning to the nonequilibrium setup.

As illustrated in Fig. 5(b), compared to the equilibrium case with $\Delta\mu = 0$, signifi-
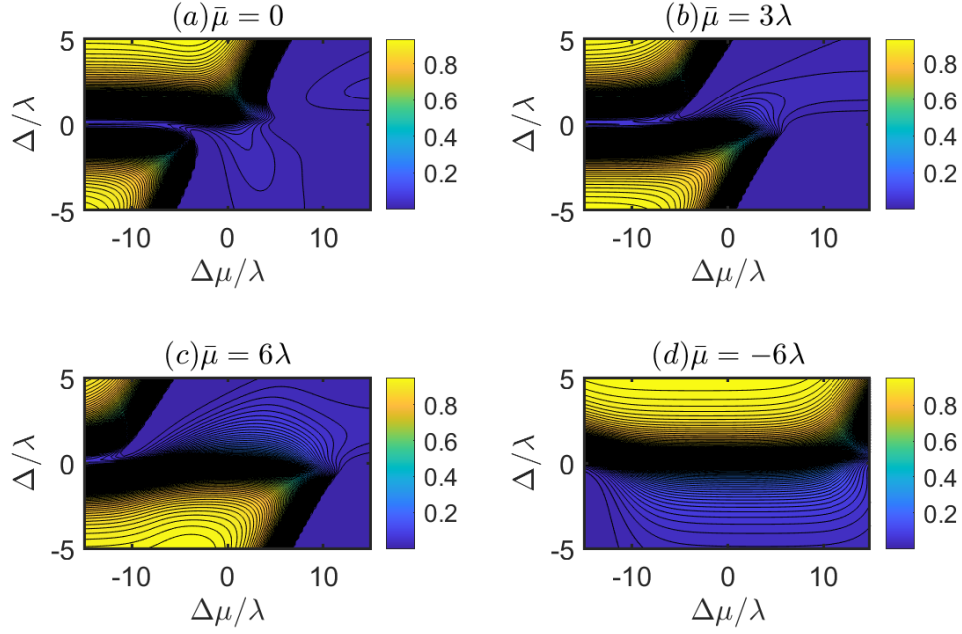
Figure 4: The efficiency R_{ss} as a function of the chemical potential difference $\Delta\mu$ and the detuning Δ for nonequilibrium fermion reservoirs. The parameters are set as $F = 0.5\lambda$, $\omega_c = 5\lambda$, $T_1 = T_2 = \lambda$, $\bar{\Delta} = 0$, and $\alpha_1 = \alpha_2 = 0.1\lambda$.
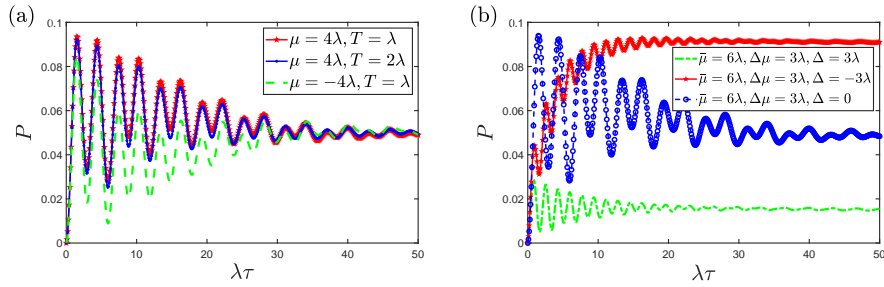
Figure 5: The charging power $P(\tau) = E(\tau)/\tau$ in the equilibrium and nonequilibrium fermion reservoirs. The parameters are set as $\mu_1 = \mu_2 = \mu$, $T_1 = T_2 = T$, $F = 0.5\lambda$, $\omega_c = 5\lambda$, $\Delta_1 = \Delta_2 = 0$, $\alpha_1 = \alpha_2 = 0.1\lambda$ for (a) and $T_1 = T_2 = \lambda$, $F = 0.5\lambda$, $\omega_c = 5\lambda$, $\bar{\Delta} = 0$, $\alpha_1 = \alpha_2 = 0.1\lambda$ for (b).

cantly higher charging power can be achieved for $\Delta\mu > 0$ in the regime $\Delta < 0$. This highlights the pivotal role of the compensation mechanism in enhancing the charging power in a nonequilibrium quantum battery setup.

6 Conclusion

In this paper, we have investigated the efficiency of a quantum battery setup where both the charger and the battery are modeled as two-level systems. These systems are coherently coupled to each other and simultaneously interact with their respective fermionic reservoirs, with nonequilibrium characterized by the chemical potential difference. Going beyond the traditional phenomenological master equation, we consider the effects of external driving and charger-battery coupling on the eigen spectrum of the system. By treating these effects in a non-perturbative manner, we derive the Redfield master equation without applying the secular approximation. Solving this master equation, we reveal the significant role of nonequilibrium reservoirs in the performance of the quantum battery setup. Generally, the Redfield master equation does not guarantee the positivity of the density matrix, as the eigen values of the density matrix may become negative. However, we have verified that the density matrix remains positive throughout the entire parameter regime considered in this study. Our results demonstrate that when the charger is driven non-resonantly, the chemical potential difference in the fermionic reservoirs can enhance the quantum battery's efficiency via a compensation mechanism. This mechanism is particularly effective under non-resonant driving and can also be employed to boost the charging power of the quantum battery under significant nonequilibrium conditions. In summary, nonequilibrium reservoirs provide an effective framework for designing energy devices based on open quantum systems.

Author contributions   Z. Wang and J. Wang designed the research. Z. Wang and H. Yu performed the main calculations. Z. Wang and J. Wang wrote the manuscript. All of the authors contributed to the planning and made revision of the manuscript.

Funding information   Science and Technology Development Project of Jilin Province (Grant No. 20230101357JC) and National Natural Science Foundation of China (Grants No. 12375010, 21721003 and 12234019).

References

[1] R. Alicki and M. Fannes, *Entanglement boost for extractable work from ensembles of quantum batteries*, Phys. Rev. E **87**, 042123 (2013), doi: 10.1103/PhysRevE.87.042123

[2] T. P. Le, J. Levinsen, K. Modi, M. M. Parish and F. A. Pollock, *Spin-chain model of a many-body quantum battery*, Phys. Rev. A **97**, 022106 (2018), doi: 10.1103/PhysRevA.97.022106

[3] D. Ferraro, M. Campisi, G. M. Andolina, V. Pellegrini and M. Polini, *High-power collective charging of a solid-state quantum battery*, Phys. Rev. Lett. **120**, 117702 (2018), doi: 10.1103/PhysRevLett.120.117702

[4] D. Rossini and E. Vicari, *Scaling of decoherence and energy flow in interacting quantum spin systems*, **Phys. Rev. A 99, 052113 (2019), doi: 10.1103/PhysRevA.99.052113**

[5] Y.-Y. Zhang, T.-Ran Yang, L. Fu and X. Wang, *Powerful harmonic charging in a quantum battery*, **Phys. Rev. E 99, 052106 (2019), doi: 10.1103/PhysRevE.99.052106**

[6] J. Chen, L. Zhan, L. Shao, X. Zhang, Y. Zhang and X. Wang, *Charging quantum batteries with a general harmonic driving field*, **ANNALEN DER PHYSIK 532, 1900487 (2020), doi: 10.1002/andp.201900487**

[7] D. Rossini, G. M. Andolina, D. Rosa, M. Carrega and M. Polini, *Quantum advantage in the charging process of Sachdev-Ye-Kitaev batteries*, **Phys. Rev. Lett. 125, 236402 (2020), doi: 10.1103/PhysRevLett.125.236402**

[8] Z. Li, P. Yang, W.-L. You and N. Wu, *Dynamics of the homogeneous two-qubit XXZ central spin model with the spin bath prepared in superpositions of symmetric Dicke states*, **Phys. Rev. A 102, 032409 (2020), doi: 10.1103/PhysRevA.102.032409**

[9] S. Ghosh, T. Chanda and A. Sen, *Enhancement in the performance of a quantum battery by ordered and disordered interactions*, **Phys. Rev. A 101, 032115 (2020), doi: 10.1103/PhysRevA.101.032115**

[10] V. P. Patil, Z. Kos, M. Ravnik and J. Dunkel, *Discharging dynamics of topological batteries*, **Phys. Rev. Research 2, 043196 (2020), doi: 10.1103/PhysRevResearch.2.043196**

[11] F. Caravelli, B. Yan, L. Pedro, G. Pintos and A. Hamma, *Energy storage and coherence in closed and open quantum batteries*, **Quantum 5, 505 (2021), doi: 10.22331/q-2021-07-15-505**

[12] F. Zhao, F.-Q. Dou and Q. Zhao, *Quantum battery of interacting spins with environmental noise* **Phys. Rev. A 103, 033715 (2021), doi: 10.1103/PhysRevA.103.033715**

[13] O. Abah, G. D. Chiara, M. Paternostro and R. Puebla, *Harnessing nonadiabatic excitations promoted by a quantum critical point: Quantum battery and spin squeezing*, **Phys. Rev. Research 4, L022017 (2022), doi: 10.1103/PhysRevResearch.4.L022017**

[14] F. Zhao, F.-Q. Dou and Q. Zhao, *Charging performance of the Su-Schrieffer-Heeger quantum battery*, **Phys. Rev. Research 4, 013172 (2022), doi: 10.1103/PhysRevResearch.4.013172**

[15] Y. Yao and X. Q. Shao, *Optimal charging of open spin-chain quantum batteries via homodyne-based feedback control*, **Phys. Rev. E 106, 014138 (2022), doi: 10.1103/PhysRevE.106.014138**

[16] L. Fusco, M. Paternostro and G. D. Chiara, *Work extraction and energy storage in the Dicke model*, **Phys. Rev. E 94, 052122(2016), doi: 10.1103/PhysRevE.94.052122**

[17] G. M. Andolina, M. Keck, A. Mari, V. Giovannetti and M. Polini, *Quantum versus classical many-body batteries*, **Phys. Rev. B 99, 205437 (2019), doi: 10.1103/PhysRevB.99.205437**

[18] D. Z. Rossatto, D. P. Pires, F. M. de Paula and O. P. de SaNeto, *Quantum coherence and speed limit in the mean-field Dicke model of superradiance*, **Phys. Rev. A 102, 053716 (2020), doi: 10.1103/PhysRevA.102.053716**

[19] A. Crescente, M. Carrega, M. Sassetti and D. Ferraro, *Ultrafast charging in a two-photon Dicke quantum battery*, **Phys. Rev. B 102, 245407 (2020), doi: 10.1103/Phys-RevB.102.245407**

[20] W. Lu, J. Chen, L.-M. Kuang and X. Wang, *Optimal state for a Tavis-Cummings quantum battery via the Bethe ansatz method*, **Phys. Rev. A 104, 043706 (2021), doi: 10.1103/PhysRevA.104.043706**

[21] F.-Q. Dou, Y.-Q. Lu, Y.-J. Wang and J.-A. Sun, *Extended Dicke quantum battery with interatomic interactions and driving field*, **Phys. Rev. B 105, 115405 (2022), doi: 10.1103/PhysRevB.105.115405**

[22] Y. Yao and X. Q. Shao, *Stable charging of a Rydberg quantum battery in an open system*, **Phys. Rev. E 104, 044116 (2021), doi: 10.1103/PhysRevE.104.044116**

[23] S-Y. Bai and J.-H. An, *Floquet engineering to reactivate a dissipative quantum battery*, **Phys. Rev. A 102, 060201 (2020), doi: 10.1103/PhysRevA.102.060201**

[24] S.-Y. Bai, C. Chen, H. Wu and J.-H. An, *Quantum control in open and periodically driven systems*, **Advances in Physics: X 6, 1870559 (2021), doi: 10.1080/23746149.2020.1870559**

[25] S. Mondal and S. Bhattacharjee, *Periodically driven many-body quantum battery*, **Phys. Rev. E 105, 044125 (2022), doi: 10.1103/PhysRevE.105.044125**

[26] F. Barra, *Dissipative charging of a quantum battery*, **Phys. Rev. Lett. 122, 210601 (2019), doi: 10.1103/PhysRevLett.122.210601**

[27] C. L. Latune, I. Sinayskiy and F. Petruccione, *Heat flow reversals without reversing the arrow of time: The role of internal quantum coherences and correlations*, **Phys. Rev. Research 1, 033097 (2019), doi: 10.1103/PhysRevResearch.1.033097**

[28] D. Farina, G. M. Andolina, A. Mari, M. Polini and V. Giovannetti, *Charger-mediated energy transfer for quantum batteries: An open-system approach*, **Phys. Rev. B 99, 035421 (2019), doi: 10.1103/PhysRevB.99.035421**

[29] A. Crescente, M. Carrega, M. Sassetti and D. Ferraro, *Charging and energy fluctuations of a driven quantum battery*, **New J. Phys. 22, 063057(2020), doi: 10.1088/1367-2630/ab91fc**

[30] M. Carrega, A. Crescente, D. Ferraro and M. Sassetti, *Dissipative dynamics of an open quantum battery*, **New J. Phys. 22, 083085 (2020), doi: 10.1088/1367-2630/abaa01**

[31] F. H. Kamin, F. T. Tabesh, S. Salimi, F. Kheirandish and A. C. Santos, *Non-Markovian effects on charging and self-discharging process of quantum batteries*, **New J. Phys. 22, 083007 (2020), doi: 10.1088/1367-2630/ab9ee2**

[32] F. T. Tabesh, F. H. Kamin and S. Salimi, *Environment-mediated charging process of quantum batteries*, **Phys. Rev. A 102, 052223 (2020), doi: 10.1103/PhysRevA.102.052223**

[33] F. Tacchino, T. F. F. Santos, D. Gerace, M. Campisi and M. F. Santos, *Charging a quantum battery via nonequilibrium heat current*, **Phys. Rev. E 102, 062133 (2020), doi: 10.1103/PhysRevE.102.062133**

[34] W. Chang, T.-R. Yang, H. Dong, L. Fu, X. Wang and Y.-Y. Zhang, *Optimal building block of multipartite quantum battery in the driven-dissipative charging*, **New J. Phys. 23, 103026 (2021)**, doi: 10.1088/1367-2630/ac2a5b

[35] K. Xu, H.-J. Zhu, G.-F. Zhang and W.-M. Liu, *Enhancing the performance of an open quantum battery via environment engineering*, **Phys. Rev. E 104, 064143 (2021)**, doi: 10.1103/PhysRevE.104.064143

[36] F. Mayo and A. J. Roncaglia, *Collective effects and quantum coherence in dissipative charging of quantum batteries*, **Phys. Rev. A 105, 062203 (2022)**, doi: 10.1103/PhysRevA.105.062203

[37] H. P. Breuer and F. Petruccione, *The Theory of Open Quantum Systems* (Oxford University Press, Oxford, 2007).

[38] F. Bloch, *Generalized theory of relaxation*, **Phys. Rev. 105, 1206 (1957)**, doi: 10.1103/PhysRev.105.1206

[39] A. G. Redfield, *On the theory of relaxation processes*, **IBM J. Res. Dev. 1, 19 (1957)**, doi: 10.1147/rd.11.0019

[40] A. Ishizaki and G. R. Fleming, *On the adequacy of the Redfield equation and related approaches to the study of quantum dynamics in electronic energy transfer*, **J. Chem. Phys. 130, 234110 (2009)**, doi: 10.1063/1.3155214

[41] C. K. Lee, J. Moix and J. Cao, *Coherent quantum transport in disordered systems: A unified polaron treatment of hopping and band-like transport*, **J. Chem. Phys. 142, 164103 (2015)**, doi: 10.1063/1.4918736

[42] V. I. Novoderezhkin, A. G. Yakovlev, R. van Grondelle and V. A. Shuvalov, *Coherent nuclear and electronic dynamics in primary charge separation in photosynthetic reaction centers: a Redfield theory approach*, **J. Phys. Chem. B 108, 7445 (2004)**, doi: 10.1021/jp0373346

[43] J. Jeske, D. J. Ing, M. B. Plenio, S. F. Huelga and J. H. Cole, *Bloch-Redfield equations for modeling light-harvesting complexes*, **J. Chem. Phys. 142, 064104 (2015)**, doi: 10.1063/1.4907370

[44] M.-J. Tao, N.-N. Zhang, P.-Y. Wen, F.-G. Deng, Q. Ai and G.-L. Long, *Coherent and incoherent theories for photosynthetic energy transfer*, **Sci. Bull. 65, 318 (2020)**, doi: 10.1016/j.scib.2019.12.009

[45] Z. D. Zhang and J. Wang, *Curl flux, coherence, and population landscape of molecular systems: Nonequilibrium quantum steady state, energy (charge) transport, and thermodynamics*, **J. Chem. Phys. 140, 245101 (2014)**, doi: 10.1063/1.4884125

[46] S.-W. Li, C. Y. Cai and C. P. Sun, *Steady quantum coherence in non-equilibrium environment*, **Ann. Phys. 360, 19 (2015)**, doi: 10.1016/j.aop.2015.05.004

[47] Y. Huangfu and J. Jing, *Steady bipartite coherence induced by non-equilibrium environment*, **Sci. China-Phys. Mech. Astron. 61, 010311 (2018)**, doi: 10.1007/s11433-017-9115-2

[48] Z. D. Zhang and J. Wang, *Landscape, kinetics, paths and statistics of curl flux, coherence, entanglement and energy transfer in non-equilibrium quantum systems*, **New J. Phys. 17, 043053 (2015)**, doi: 10.1088/1367-2630/17/4/043053

[49] Z. D. Zhang and J. Wang, *Shape, orientation and magnitude of the curl quantum flux, the coherence and the statistical correlations in energy transport at nonequilibrium steady state*, **New J. Phys. 17, 093021 (2015), doi: 10.1088/1367-2630/17/9/093021**

[50] Z. Wang, W. Wu, G. Cui and J. Wang, *Coherence enhanced quantum metrology in a nonequilibrium optical molecule*, **New J. Phys. 20, 033034 (2018), doi: 10.1088/1367-2630/aab03a**

[51] G. Guarnieri, M. Kolar and R. Filip, *Steady-state coherences by composite system-bath interactions*, **Phys. Rev. Lett. 121, 070401 (2018), doi: 10.1103/PhysRevLett.121.070401**

[52] Z. Wang, W. Wu and J. Wang, *Steady-state entanglement and coherence of two coupled qubits in equilibrium and nonequilibrium environments*, **Phys. Rev. A 99, 042320 (2019), doi: 10.1103/PhysRevA.99.042320**

[53] L.-B. Fan, Y.-H. Zhou, F. Zou, H. Guo, J.-F. Huang and J.-Q. Liao, *Quantum thermalization and vanishing thermal entanglement in the open Jaynes-Cummings model*, **ANNALEN DER PHYSIK 532, 2000134 (2020), doi: 10.1002/andp.202000134**

[54] B. Mojaveri, A. Dehghani and Z. Ahmadi, *Maximal steady-state entanglement and perfect thermal rectification in non-equilibrium interacting XXZ chains*, **Eur. Phys. J. Plus 136, 83 (2021), doi: 10.1140/epjp/s13360-020-01016-0**

[55] Y. Khlifi, S. Seddik and A. El Allati, *Steady state entanglement behavior between two quantum refrigerators*, **Physica A: Statistical Mechanics and its Applications 596, 127199 (2022), doi: 10.1016/j.physa.2022.127199**

[56] A. E. Allahverdyan, R. Balian and T. M. Nieuwenhuizen, *Maximal work extraction from finite quantum systems*, **Europhys. Lett. 67, 565 (2004), doi: 10.1209/epl/i2004-10101-2**

[57] W. Pusz and S. L. Woronowicz, *Passive states and KMS states for general quantum systems*, **Commun. Math. Phys. 58, 273 (1978), doi: 10.1007/BF01614224**

[58] W. K. Wootters, *Entanglement of formation of an arbitrary state of two qubits*, **Phys. Rev. Lett. 80, 2245 (1998), doi: 10.1103/PhysRevLett.80.2245**